FIGURE 6. VV-IL-23-infected lymphocytes produce both IFN-γ and IL-17. A and B, Naive spleen cells of BALB/c mice were infected in vitro with VV-WT (WT), VV-IL-12 (IL-12), or VV-IL-23 (IL-23). Noninfected spleen cells (None) were used as a negative control. C and D, Naive spleen cells of BALB/c mice were cultured with either recombinant IL-12 or recombinant IL-23 at various concentrations. After 2 days of incubation, amounts of IFN-γ (A and C) and IL-17 (B and D) in the culture supernatants were quantitated by ELISA. Data are shown as the mean ± SEM of three to five mice per group. The experiment was repeated three times with similar results. ND, Not detected. *, $p < 0.01$.

mice were measured after inoculation of a sublethal dose (5×10^6 PFU) of VV (Fig. 7B). Both VV-IL-12-infected and VV-IL-23-infected IL-12/23p40 KO mice almost cleared the virus at day 14 postinfection, although high virus titers were retained in VV-WT-inoculated IL-12/23p40 KO mice on the same day (Fig. 7B). Taken together, IL-23 delivered by VV-IL-23 is capable of enhancing the resistance to VV independently of IL-12 and vice versa. Based on the data of viral titers at day 21 postinfection with VV-WT (Fig. 7C), it was confirmed that IL-12/23p40 KO mice were far more sensitive to VV infection than were BALB/c mice, indicating that IL-12 and/or IL-23 play a critical role in resistance to VV infection. VV-IL-12-infected spleen cells of IL-12/23p40 KO mice produced IFN-γ as much as those of BALB/c mice (Fig. 7D), indicating that IL-12 delivered by VV-IL-12 efficiently stimulated to produce IFN-γ even in the absence of IL-12/23p40. In contrast, VV-IL-23-infected spleen cells derived from IL-12/23p40 KO mice secreted significant amounts of both IFN-γ (Fig. 7D) and IL-17 (Fig. 7E) as well as VV-IL-23-infected BALB/c spleen cells.
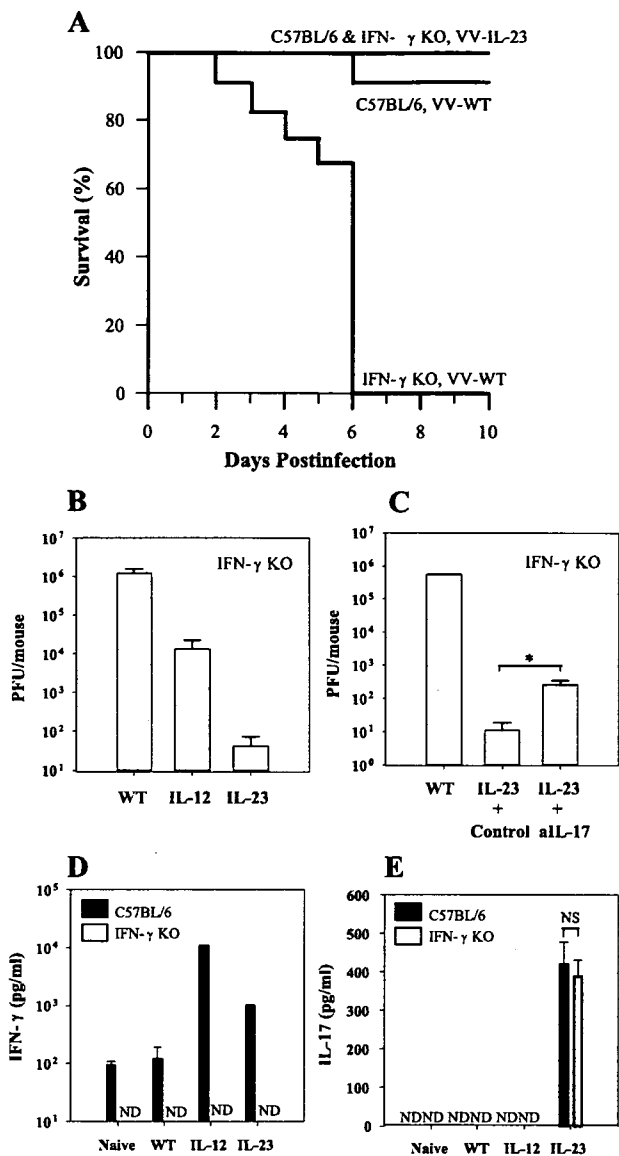
IL-23 enhanced the resistance to VV in IFN-γ-deficient mice

We then investigated the host defense against VV-IL-23 in the absence of IFN-γ. IFN-γ KO mice of the C57BL/6 background and control mice (C57BL/6) were infected with 2×10^8 PFU/mouse of either VV-WT or VV-IL-23 for monitoring survival rates (Fig. 8A). Because C57BL/6 mice are more resistant to VV than BALB/c mice (M. Matsui, unpublished observations), it is understandable that only one of eight C57BL/6 mice infected with VV-WT died, and all C57BL/6 mice ($n = 8$) infected with VV-IL-23 survived the infection. In contrast, all IFN-γ KO mice ($n = 12$) succumbed to the infection with VV-WT by day 6 postinfec-
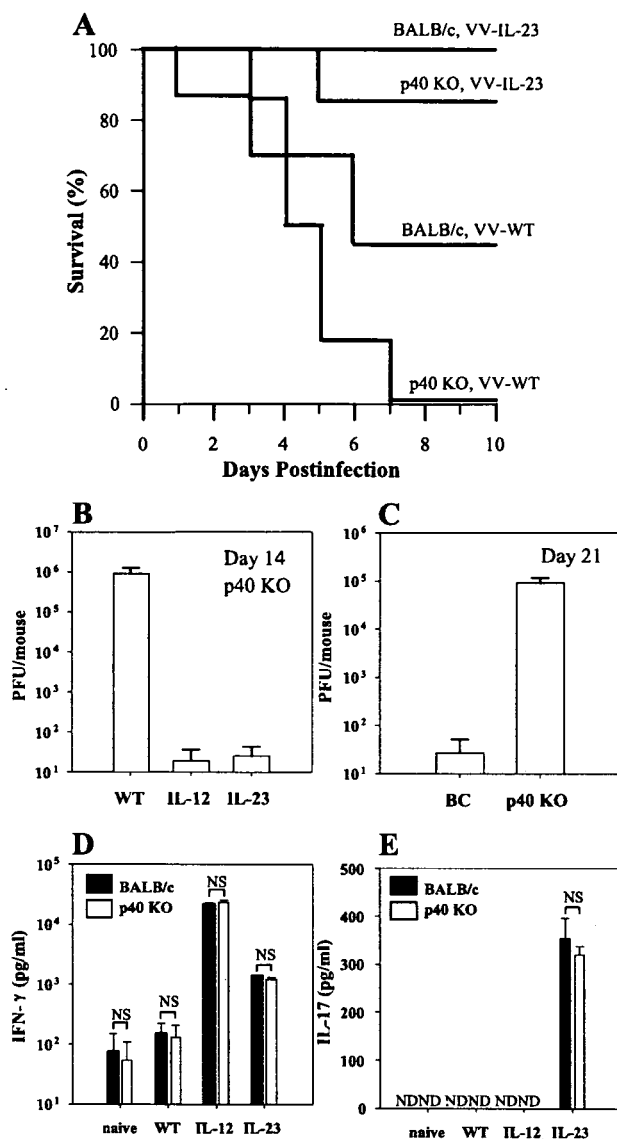

FIGURE 7. IL-23 delivered by VV-IL-23 enhances resistance to VV infection in IL-12/23p40-deficient mice. A, IL-12/23p40-deficient mice and BALB/c mice were infected i.p. with 2×10^8 PFU of VV-WT or VV-IL-23, and were monitored daily for mortality. B, IL-12/23p40-deficient mice infected with 5×10^6 PFU of VV-WT (WT), VV-IL-12 (IL-12), or VV-IL-23 (IL-23) were sacrificed at day 14 postinfection, and viral titers in ovaries were measured. From 8 to 12 mice were used in each group, and all titrations were performed in duplicates. Data are shown as the mean PFU ± SEM. C, BALB/c mice (BC) and IL-12/23p40-deficient mice (p40 KO) were infected with 5×10^6 PFU of VV-WT and sacrificed at day 21 postinfection. Viral titers in ovaries were then measured. Data shown are the mean PFU ± SEM. D and E, Naive spleen cells of either BALB/c or IL-12/23p40-deficient (p40 KO) mice were infected in vitro with VV-WT (WT), VV-IL-12 (IL-12), or VV-IL-23 (IL-23). Noninfected spleen cells (Naive) were used as a negative control. After 2 days of incubation, culture supernatants were screened for the presence of IFN-γ (D) and IL-17 (E) by ELISA. Data are shown as the mean ± SEM of three to five mice per group. Each experiment was repeated three times with similar results. ND, Not detected.

tion, indicating that IFN-γ plays a crucial role in resistance to VV infection. However, all IFN-γ KO mice ($n = 8$) survived the infection with VV-IL-23, showing that IL-23 delivered by VV-IL-23 enhances the host defense against VV infection even in the

FIGURE 8. IL-23 delivered by VV-IL-23 enhances resistance to VV infection in IFN-γ-deficient mice. *A*, IFN-γ-deficient (IFN-γ KO) mice and C57BL/6 mice were infected i.p. with 2 × 10⁸ PFU of VV-WT or VV-IL-23, and were monitored daily for mortality. *B*, IFN-γ-deficient mice infected with 5 × 10⁶ PFU of VV-WT (WT), VV-IL-12 (IL-12), or VV-IL-23 (IL-23) were sacrificed at day 14 postinfection, and viral titers in ovaries were measured. Six to twelve mice were used in each group. and all titrations were performed in duplicates. Data are shown as the mean PFU ± SEM. *C*, IFN-γ -deficient mice were infected with 5 × 10⁶ PFU of VV-WT (WT) or VV-IL-23 (IL-23). VV-IL-23-infected mice were then administered with 70 μg of a neutralizing anti-IL-17 mAb (aIL-17) or a relevant isotype control Ab (Control) at days 0, 2, 7 postinfection with VV. Viral titers in ovaries were then measured at day 14 postinfection. Four mice were used in each group, and all titrations were performed in duplicates. Data are shown as the mean PFU ± SEM. *, *p* < 0.01. *D* and *E*, Naive spleen cells of either C57BL/6 or IFN-γ-deficient (IFN-γ KO) mice were infected in vitro with VV-WT (WT), VV-IL-12 (IL-12), or VV-IL-23 (IL-23). Noninfected spleen cells (Naive) were used as a negative control. After 2 days of incubation, culture supernatants were screened for the presence of IFN-γ (*D*) and IL-17 (*E*) by ELISA. Data are shown as the mean± SEM of three to five mice per group. The experiment was repeated three times with similar results. ND, Not detected.
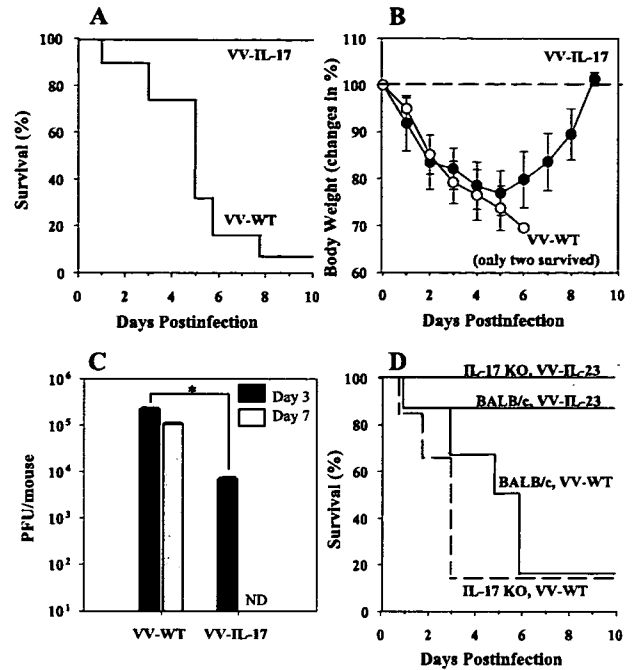
FIGURE 9. Role of IL-17 in resistance to VV infection. *A* and *B*, Twelve BALB/c mice per group were infected i.p. with 5 × 10⁸ PFU of VV-WT or VV-IL-17. *A*, Mice were monitored daily for mortality. *B*, Changes in body weight of mice infected with VV-WT (open symbols) or VV-IL-17 (solid symbols) were calculated as the percentage of the mean weight per group in comparison with starting body weight. Data are shown as the mean ± SEM. *C*, BALB/c mice infected with 5 × 10⁶ PFU of VV-WT or VV-IL-17 were sacrificed at day 3 (■) or 7 (▣) postinfection, and virus titers in ovaries of mice were measured. Six mice were used in each group, and all titrations were performed in duplicates. Data are shown as the mean PFU ± SEM. Nd, Not detected. *, *p* < 0.01. *D*, IL-17-deficient (IL-17 KO) mice and BALB/c mice were infected i.p. with 5 × 10⁸ PFU of VV-WT or VV-IL-23, and were monitored daily for mortality. Six mice were used in each group. Data of VV-WT-infected IL-17 KO mice were shown as a dashed line for highlighting.

absence of IFN-γ. Viral titers in ovaries of IFN-γ KO mice were then examined after inoculation of a sublethal dose of VV (Fig. 8*B*). It was confirmed that C57BL/6 mice did not resolve VV-WT in ovaries, but did eliminate VV-IL-23 as well as VV-IL-12 at day 14 postinfection in the same manner as BALB/c mice (data not shown). In accordance with the survival data (Fig. 8*A*), IFN-γ KO mice nearly cleared VV-IL-23 in ovaries at day 14 postinfection, whereas high virus titers were still retained in ovaries of IFN-γ KO mice inoculated with either VV-WT or VV-IL-12 (Fig. 8*B*). These data indicate that IL-23 promotes resistance to VV even in the absence of IFN-γ and strongly suggest that the mechanism of the IL-23-mediated resistance to VV infection is distinct from that of the IL-12-regualted resistance in which IFN-γ plays a critical role. It was reported that IL-17 plays a critical role in the IL-23-dependent resistance to bacteria such as *K. pneumoniae* (17) and *C. rodentium* (11). To examine contribution of IL-17 in the IL-23-mediated resistance. VV-IL-23-infected IFN-γ KO mice were administered with a neutralizing anti-IL-17 mAb. As shown in Fig. 8*C*. treatment with the anti-IL-17 mAb, but not with a control mAb, resulted in a slight but significant increase of viral titers in ovaries at day 14 postinfection, suggesting an involvement of IL-17 in the IL-23-associated host defense against VV in the absence of IFN-γ. It was confirmed that spleen cells of IFN-γ KO

mice infected with VV-WT, VV-IL-12, or VV-IL-23 did not produce IFN-γ at all (Fig. 8D). In contrast, VV-IL-23-infected spleen cells of IFN-γ KO mice produced IL-17 as much as VV-IL-23-infected spleen cells of C57BL/6 mice (Fig. 8E).

Role of IL-17 in resistance to VV infection

To further examine the role of IL-17 in resistance to VV infection, we have constructed VV-IL-17 and investigated the susceptibility of BALB/c mice to VV-IL-17. It was confirmed that IL-17 was detected in the culture supernatant of VV-IL-17-infected 293T cells by ELISA, and IL-17 in the culture supernatant could induce IL-6 production from NIH 3T3 cells (data not shown). BALB/c mice were injected i.p. with 5×10^8 PFU/mouse of either VV-WT or VV-IL-17 for monitoring survival rates (Fig. 9A) and changes in body weight (Fig. 9B). As shown in Fig. 9B, VV-IL-17-infected mice looked very sick on the first few days after infection, but all of the mice ($n = 12$) eventually recovered from illness (Fig. 9A and B). In contrast, eleven of twelve mice injected with VV-WT succumbed to the infection (Fig. 9, A and B). Furthermore, VV-IL-17-infected BALB/c mice cleared VV from ovaries at day 7 postinfection with 5×10^6 PFU, whereas VV-WT-infected mice did not clear the virus (Fig. 9C). These results demonstrate that IL-17 promotes host resistance to VV infection, and therefore, support the data in Fig. 8C showing an involvement of IL-17 in the IL-23-mediated defense against VV. We next tested resistance to VV-WT and VV-IL-23 in IL-17-deficient mice. BALB/c mice and IL-17 KO mice of the BALB/c background were infected i.p. with 5×10^8 PFU/mouse of either VV-WT or VV-IL-23 and were monitored for mortality. As shown in Fig. 9D, IL-17 KO mice were more sensitive to VV-WT than control BALB/c mice, showing that IL-17 is necessary for host defense against VV infection. In contrast, all of VV-IL-23-infected IL-17 KO mice survived the infection, indicating that IL-17 is dispensable for the IL-23-mediated clearance of VV.

Discussion

In the current study, we demonstrated that IL-23 delivered by VV-IL-23 enhanced resistance to VV infection in BALB/c mice as well as IL-12 (Fig. 2). A similar activity of IL-23 was observed in IL-12/23p40-deficient mice infected with VV-IL-23 as well (Fig. 7, A and B), indicating that IL-23 enhances resistance to VV infection independently of IL-12. In other words, IL-23 could compensate for the lack of IL-12 in the host defense against VV. However, the mechanism of the IL-23-mediated resistance to VV infection is different from that of the IL-12-regulated resistance because IFN-γ-deficient mice did not eliminate VV-IL-12, but almost did eradicate VV-IL-23 in ovaries at day 14 postinfection (Fig. 8B). VV-IL-23-infected cells produced a certain amount of IFN-γ (Fig. 6A), and furthermore, several early studies pointed out that IL-23 stimulated the production of IFN-γ to induce various immune responses including CTL responses (2, 5, 6, 31). However, the current data indicate that IFN-γ is dispensable for the IL-23-regulated resistance to VV, although it does not mean that IFN-γ induced by IL-23 is totally useless in resistance to VV infection. According to the survival rate of IFN-γ KO mice infected with VV-WT (Fig. 8A), IFN-γ plays a critical role in host defense against VV infection, and hence, IL-23-induced IFN-γ should be beneficial for the viral clearance. Rather, it is possible to assume that some other factors could play a dominant role and compensate for the absence of IFN-γ in the IL-23-regulated resistance to VV. In contrast, IFN-γ plays a critical role in the IL-12-mediated resistance to VV (Fig. 8B). In fact, VV-IL-12-infected cells secreted large amounts of IFN-γ (Fig. 6A). However, viral titers of VV-IL-12-infected IFN-γ KO

mice were ~100 times lower than those of VV-WT-infected IFN-γ KO mice (Fig. 8B). This finding could be explained by the IFN-γ-independent activity of IL-12 including direct effects on T cells and NK cells acting as a growth factor and an enhancer of cytotoxicity as well as inducing other cytokines (32).

Because the IL-23/IL-17 axis is known to be required for the host protection against *K. pheumoniae* (17) and *C. rodentium* (11), and further VV-IL-23-infected cells produced considerable amounts of IL-17 (Fig. 6B), it was quite possible to expect that IL-17 might play a major role in the IL-23-regulated resistance to VV infection. In fact, treatment with a neutralizing anti-IL-17 mAb resulted in a significant increase of viral titers in ovaries of VV-IL-23-infected IFN-γ KO mice (Fig. 8C), suggesting an involvement of IL-17 in the IL-23-regulated defense against VV at least in the absence of IFN-γ. It is presumed that the anti-viral IL-17 was secreted from Th17 cells, which were differentiated by TGF-β and IL-6 and were expanded to acquire fully effective function by IL-23 (10–12). However, the effect of neutralization with anti-IL-17 mAb was limited (Fig. 8C) although we cannot rule out the possibility that IL-17 in the mice was not fully neutralized with the mAb. These data suggest that something else directly or indirectly induced by IL-23 should play a major role in the IL-23-regulated resistance to VV infection. For example, it has recently been reported that Th17 cells secrete IL-22 together with IL-17 (33, 34). IL-22 in conjunction with IL-17 synergistically functions in host defense as well as in the pathogenesis of autoimmune diseases (33, 34). Actually, activated T cells from HIV-1-exposed, but uninfected individuals overproduce IL-22, suggesting that IL-22 participates in an innate anti-HIV-1 host resistance (35). It might be possible to presume that IL-22 is associated with the IL-23-driven enhancement of the resistance to VV. In addition, a potent inflammatory cytokine, IL-17F might play a major role in the IL-23-mediated resistance because Th17 cells produce IL-17F (36) as well as IL-17 (IL-17A) and IL-22.

To test whether IL-17 participates in host defense against VV infection, we have engineered VV-IL-17 and compared it with VV-WT. As shown in Fig. 9, A–C, VV-IL-17 was less virulent than VV-WT in BALB/c mice, indicating that IL-17 promotes resistance to VV infection. It has been reported that the IL-23/Th17/IL-17 axis plays an essential role in neutrophil recruitment (37). In the case of influenza virus infection, neutrophils as well as macrophages are accumulated at the site of infection soon after the viral infection, and either type of cell is capable of phagocytosing virus-infected, apoptotic cells (38). Virus-infected, apoptotic cells phagocytosed are then digested together with virus by degrading enzymes that exist in lysosomes of phagocytes. Hence, the influx of neutrophils induced by IL-17 may contribute to the rapid clearance of VV in VV-IL-17-infected mice. In the current study, VV-IL-17 induced viral clearance by day 7 of infection (Fig. 9C), whereas VV-IL-23 took 14 days to clear the virus (Fig. 2C). It may be possible to assume that VV-IL-17-infected cells could secrete large amounts of IL-17 at the site of infection faster than VV-IL-23-infected cells, and thereby, could induce the rapid influx of neutrophils, which may lead to the faster clearance of the virus. In addition, IL-17 KO mice were likely to be more sensitive to VV-WT than BALB/c mice (Fig. 9D), indicating that IL-17 is important in host defense against VV. However, IL-17 KO mice survived the infection with VV-IL-23 (Fig. 9D), demonstrating that IL-17 does not play a dominant role in the IL-23-regulated resistance to VV infection. Taken together, IL-23 may be working in the resistance to VV predominately through other effector molecules expressed by Th17 cells such as IL-22 or IL-17F although IL-17 (IL-17A) is likely to play at least a certain role in the IL-23-mediated resistance to VV.

It was previously shown that IL-23 and the subsequent IL-17 pathway play an essential role in resistance to infection with certain extracellular bacteria (11, 17). In contrast, Cua et al. (39) proposed that the IL-23/Th17 axis has physiologically been designed for the induction of immediate inflammatory response against catastrophic breaches of pathogens in the initial phase of mucosal infection. Our current data show a significant role of IL-23 in host defense against VV for the first time. Furthermore, IL-17 participates in the IL-23-regulated resistance to VV infection, but IL-17 is unlikely to play a dominant role in it. Our data provide a possibility that there might be an alternative pathway in the mechanism of IL-23-regulated resistance to VV infection. Therefore, our data suggest that it might be possible to use the adjuvant activity of IL-23 for the prophylactic and therapeutic strategies against infectious pathogens without side effects of autoimmunity caused by the IL-23/Th17/IL-17 axis.

Acknowledgments

Disclosures

The authors have no financial conflict of interest.

References

1. Trinchieri, G. 2003. Interleukin-12 and the regulation of innate resistance and adaptive immunity. *Nat. Rev. Immunol.* 3: 133–146.
2. Oppmann, B., R. Lesley. B. Blom. J. C. Timans, Y. Xu, B. Hunte. F. Vega, N. Yu, J. Wang. K. Singh. et al. 2000. Novel p19 protein engages IL-12p40 to form a cytokine, IL-23. with biological activities similar as well as distinct from IL-12. *Immunity* 13: 715–725.
3. Parham. C.. M. Chirica. J. Timans, E. Vaisberg, M. Travis, J. Cheung. S. Pflanz, R. Zhang. K. P. Singh. F. Vega, et al. 2002. A receptor for the heterodimeric cytokine IL-23 is composed of IL-12Rβ1 and a novel cytokine receptor subunit, IL-23R. *J. Immunol.* 168: 5699–5708.
4. Belladonna. M. L.. J.-C. Renauld. R. Bianchi. C. Vacca. F. Fallarino. C. Orabona, M. C. Fioretti, U. Grohmann, and P. Puccetti. 2002. IL-23 and IL-12 have overlapping, but distinct. effects on murine dendritic cells. *J. Immunol.* 168: 5448–5454.
5. Lo. C.-H., S.-C. Lee. P.-Y. Wu. W.-Y. Pan. J. Su, C.-W. Cheng. S. R. Roffler, B.-L. Chiang, C.-N. Lee. C.-W. Wu. and M.-H. Tao. 2003. Antitumor and antimetastatic activity of IL-23. *J. Immunol.* 171: 600–607.
6. Matsui. M., O. Moriya, M. L. Belladonna, S. Kamiya, F. A. Lemonnier, T. Yoshimoto, and T. Akatsuka. 2004. Adjuvant activities of novel cytokines, interleukine-23 (IL-23) and IL-27 for induction of hepatitis C virus-specific cytotoxic T lymphocytes in HLA-A*0201 transgenic mice. *J. Virol.* 78: 9093–9104.
7. Cua, D. J.. J. Sherlock, Y. Chen. C. A. Murphy, B. Joyce. B. Seymour. L. Lucian, W. To, S. Kwan, T. Churakova, et al. 2003. Interleukin-23 rather than interleukin-12 is the critical cytokine for autoimmune inflammation of the brain. *Nature* 421: 744–748.
8. Murphy, C. A.. C. L. Langrish, Y. Chen, W. Blumenschein, T. McClanahan, R. A. Kastelein. J. D. Sedgwick, and D. J. Cua. 2003. Divergent pro- and anti-inflammatory roles for IL-23 and IL-12 in joint autoimmune inflammation. *J. Exp. Med.* 198: 1951–1957.
9. Harrington, L. E., R. D. Hatton, P. R. Mangan. H. Turner, T. L. Murphy, K. M. Murphy, and C. T. Weaver. 2005. Interleukin 17-producing CD4$^+$ effector T cells develop via a lineage distinct from the T helper type 1 and 2 lineages. *Nat. Immunol.* 6: 1123–1132.
10. Bettelli. E.. Y. Carrier, W. Gao, T. Korn, T. B. Strom, M. Oukka. H. L. Weiner, and V. K. Kuchroo. 2006. Reciprocal developmental pathways for the generation of pathogenic effector TH17 and regulatory T cells. *Nature* 441: 235–238.
11. Mangan, P. R.. L. E. Harrington, D. B. O'Quinn. W. S. Helms, D. C. Bullard, C. O. Elson. R. D. Hatton, S. M. Wahl. T. R. Schoeb, and C. T. Weaver. 2006. Transforming growth factor-β induces development of the TH17 lineage. *Nature* 441: 231–234.
12. Veldhoen, M., R. J. Hocking. C. J. Atkins, R. M. Locksley. and B. Stockinger. 2006. TGFβ in the context of an inflammatory cytokine milieu supports de novo differentiation of IL-17-producing T cells. *Immunity* 24: 179–189.
13. Park, H., Z. Li, X. O. Yang, S. H. Chang. R. Nurieva. Y.-H. Wang. Y. Wang, L. Hood, Z. Zhu. Q. Tian. and C. Dong. 2005. A distinct lineage of CD4 T cells regulates tissue inflammation by producing interleukin 17. *Nat. Immunol.* 6: 1133–1141.
14. Kolls. J. K., and A. Linden. 2004. Interleukin-17 family members and inflammation. *Immunity* 21: 467–476.
15. Nakae, S.. A. Nambu, K. Sudo, and Y. Iwakura. 2003. Suppression of immune induction of collagen-induced arthritis in IL-17-deficient mice. *J. Immunol.* 171: 6173–6177.
16. Komiyama, Y., S. Nakae. T. Matsuki, A. Nambu. H. Ishigame. S. Kakuta, K. Sudo, and Y. Iwakura. 2006. IL-17 plays an important role in the development of experimental autoimmune encephalomyelitis. *J. Immunol.* 177: 566–573.
17. Happel. K. I., P. J. Dubin. M. Zheng, N. Ghilardi. C. Lockhart, L. J. Quinton, A. R. Odden. J. E. Shellito, G. J. Bagby, S. Nelson, and J. K. Kolls. 2005. Divergent roles of IL-23 and IL-12 in host defense against *Klebsiella pneumoniae. J. Exp. Med.* 202: 761–769.
18. Moriya. O., M. Matsui. M. Osorio. H. Miyazawa, C. M. Rice. S. M. Feinstone, S. H. Leppla. J. M. Keith. and T. Akatsuka. 2002. Induction of hepatitis C virus-specific cytotoxic T lymphocytes in mice by immunization with dendritic cells treated with an anthrax toxin fusion protein. *Vaccine* 20: 789–796.
19. Yoshimoto, T.. K. Okada, N. Morishima, S. Kamiya. T. Owaki, M. Asakawa, Y. Iwakura, F. Fukai, and J. Mizuguchi. 2004. Induction of IgG2a class switching in B cells by IL-27. *J. Immunol.* 173: 2479–2485.
20. Magram, J., S. E. Connaughton, R. R. Warrier, D. M. Carvajal, C. Y. Wu, J. Ferrante. C. Stewart, U. Sarmiento, D. A. Faherty, and M. K. Gately. 1996. IL-12-deficient mice are defective in IFN-γ production and type 1 cytokine responses. *Immunity* 4: 471–481.
21. Tagawa. Y., K. Sekikawa, and Y. Iwakura. 1997. Suppression of Concanavalin A induced hepatitis in IFN-$\gamma^{-/-}$ mice. but not in TNF-$\alpha^{-/-}$ mice: role for IFN-γ in activating apoptosis of hepatocytes. *J. Immunol.* 159: 1418–1428.
22. Nakae, S., Y. Komiyama. A. Nambu, K. Sudo, M. Iwase. I. Homma, K. Sekikawa, M. Asano. and Y. Iwakura. 2002. Antigen-specific T cell sensitization is impaired in IL-17-deficient mice. causing suppression of allergic cellular and humoral responses. *Immunity* 17: 375–387.
23. Matsui. M., O. Moriya, T. Yoshimoto. and T. Akatsuka. 2005. T-bet is required for protection against vaccinia virus infection. *J. Virol.* 79: 12798–12806.
24. Yao. Z., W. C. Fanslow. F. F. Seldin, A. M. Rousseau. S. L. Painter, M. R. Comeau, J. I. Cohen, and M. K. Spriggs. 1995. *Herpesvirus saimiri* encodes a new cytokine, IL-17, which binds to a novel cytokine receptor. *Immunity* 3: 811–821.
25. Leonard, J. P., M. L. Sherman, G. L. Fisher, L. J. Buchanan, G. Larsen, M. B. Atkins, J. A. Sosman, J. P. Dutcher, N. J. Vogelzang. and J. L. Ryan. 1997. Effects of single-dose interleukin-12 exposure on interleukin-12-associated toxicity and interferon-γ production. *Blood* 90: 2541–2548.
26. Belyakov. I. M., P. Earl, A. Dzutsev. V. A. Kuznetsov, M. Lemon. L. S. Wyatt, J. T. Snyder, J. D. Ahlers, G. Franchini. B. Moss. and J. A. Berzofsky. 2003. Shared modes of protection against poxvirus infection by attenuated and conventional smallpox vaccine viruses. *Proc. Natl. Acad. Sci. USA* 100: 9458–9462.
27. Xu. R., A. J. Johnson, D. Liggitt, and M. J. Bevan. 2004. Cellular and humoral immunity against vaccinia virus infection of mice. *J. Immunol.* 172: 6265–6271.
28. Butz, E. A., and M. J. Bevan. 1998. Massive expansion of antigen-specific CD8$^+$ T cells during an acute virus infection. *Immunity* 8: 167–175.
29. Snapper. C. M., and W. E. Paul. 1987. Interferon-γ and B cell stimulatory factor-1 reciprocally regulate Ig isotype production. *Science* 236: 944–947.
30. Karupiah, G.. B. E. H. Coupar, M. E. Andrew. D. B. Boyle, S. M. Phillips, A. Mullbacher, R. V. Blanden, and I. A. Ramshow. 1990. Elevated natural killer cell responses in mice infected with recombinant vaccinia virus encoding murine IL-2. *J. Immunol.* 144: 290–298.
31. Ha, S.-J., D.-J. Kim. K.-H. Baek. Y.-D. Yun, and Y.-C. Sung. 2004. IL-23 induces stronger sustained CTL and Th1 immune responses than IL-12 in hepatitis C virus envelope protein 2 DNA immunization. *J. Immunol.* 172: 525–531.
32. Trinchieri. G. 1995. Interleukin-12 and interferon-γ: do they always go together? *Am. J. Pathol.* 147: 1534–1538.
33. Liang. S. C., X.-Y. Tan, D. P. Luxenberg, R. Karim, K. Dunussi-Joannopoulos, M. Collins. and L. A. Fouser. 2006. Interleukin (IL)-22 and IL-17 are coexpressed by Th17 cells and cooperatively enhance expression of antimicrobial peptides. *J. Exp. Med.* 203: 2271–2279.
34. Zheng. Y., D. M. Danilenko. P. Valdez, I. Kasman, J. Eastham-Anderson, J. Wu, and W. Ouyang. 2007. Interleukin-22, a TH17 cytokine, mediates IL-23-induced dermal inflammation and acanthosis. *Nature* 445: 648–651.
35. Misse. D.. H. Yssel. D. Trabattoni. C. Oblet. S. L. Caputo, F. Mazzotta. J. Pene, J.-P. Gonzalez, M. Clerici, and F. Veas. 2007. IL-22 participates in an innate nati-HIV-1 host-resistance network through acute-phase protein induction. *J. Immunol.* 178: 407–415.
36. Langrish, C. L.. Y. Chen, W. M. Blumenschein, J. Mattson, B. Basham, J. D. Sedgwick. T. McClanahan, R. A. Kastelein, and D. J. Cua. 2005. IL-23 drives a pathogenic T cell population that induces autoimmune inflammation. *J. Exp. Med.* 201: 233–240.
37. Stark, M. A., Y. Huo, T. L. Burcin, M. A. Morris. T. S. Olson, and K. Ley. 2005. Phagocytosis of apoptotic neutrophils regulates granulopoiesis via IL-23 and IL-17. *Immunity* 22: 285–294.
38. Hashimoto, Y., T. Moki, T. Takizawa, A. Shiratsuchi, and Y. Nakanishi. 2007. Evidence for phagocytosis of influenza virus-infected. apoptotic cells by neutrophils and macrophages in mice. *J. Immunol.* 178: 2448–2457.
39. Cua, D. J.. and R. A. Kastelein. 2006. TGF-β. a double agent in the immune pathology war. *Nat. Immunol.* 7: 557–559.

Intervention of MAdCAM-1 or fractalkine alleviates graft-versus-host reaction associated intestinal injury while preserving graft-versus-tumor effects

Satoshi Ueha,* Masako Murai,* Hiroyuki Yoneyama,* Masahiro Kitabatake,* Toshio Imai,[†] Takeshi Shimaoka,*,[‡] Shin Yonehara,[‡] Sho Ishikawa,* and Kouji Matsushima*,[1]

*Department of Molecular Preventive Medicine, Graduate School of Medicine, University of Tokyo, Tokyo, Japan; [†]Kan Research Institute, Kyoto, Japan; and [‡]Graduate School of Biostudies and Institute for Virus Research, Kyoto University, Kyoto, Japan

Abstract: Coincidence of the beneficial graft-vs.-tumor (GVT) effects and the detrimental graft-vs.-host disease (GVHD) remains the major obstacle against the widespread use of allogeneic bone marrow transplantation (BMT) as tumor immunotherapy. We here demonstrate that intervention of MAdCAM-1 (mucosal vascular addressin cell adhesion molecule-1) or fractalkine/CX_3CL1 after the expansion of allo-reactive donor CD8 T cells selectively inhibits the recruitment of effector donor CD8 T cells to the intestine and alleviates the graft-vs.-host reaction (GVHR) associated intestinal injury without impairing GVT effects. In a nonirradiated acute GVHD model, donor CD8 T cells up-regulate the expression of intestinal homing receptor $\alpha4\beta7$ and chemokine receptors CXCR6 and CX_3CR1, as they differentiate into effector cells and subsequently infiltrate into the intestine. Administration of anti-MAdCAM-1 antibody or anti-fractalkine antibody, even after the expansion of alloreactive donor CD8 T cells, selectively reduced the intestine-infiltrating donor CD8 T cells and the intestinal crypt cell apoptosis without affecting the induction of donor derived anti-host CTL or the infiltration of donor CD8 T cells in the hepatic tumor. Moreover, in a clinically relevant GVHD model with myeloablative conditioning, these antibodies significantly improved the survival and loss of weight without impairing the beneficial GVT effects. Thus, interruption of $\alpha4\beta7$-MAdCAM-1 or CX_3CR1-fractalkine interactions in the late phase of GVHD would be a novel therapeutic approach for the separation of GVT effects from GVHR-associated intestinal injury. *J. Leukoc. Biol.* **81: 176–185; 2007.**

Key Words: chemokines · cell trafficking · mucosa · adhesion molecule · tumor

INTRODUCTION

Despite of its limitations and toxicity, allogeneic bone marrow transplantation (allo-BMT) is now widely used as effective therapy for hematologic malignancies [1, 2]. The therapeutic benefits of allo-BMT appear to be twofold: not only can higher doses of chemo- and radiotherapy be given, but also there is the potential for graft-mediated immune response to tumors, so-called graft-vs.-tumor (GVT) effects [3, 4]. On the other hand, acute graft-vs.-host disease (GVHD) remains a serious and often fatal complication of allo-BMT. Unfortunately, the beneficial GVT effects are closely associated with adverse GVHD, because both normal tissue injuries and anti-tumor effects are mediated by donor-derived anti-host/tumor cytotoxic T lymphocytes (CTL). Administration of immunosuppressive drugs or T cell-depleted BMT improves the severity and incidence of GVHD, but these treatments often lead to the loss of anti-host/tumor CTL, resulting in the relapse of leukemia [4–6]. These observations suggest that allo-BMT would be a safe and effective immunotherapy for tumors if anti-host/tumor CTL are fully induced while normal tissues are selectively protected from anti-host/tumor CTL.

In the early phase of allo-BMT, naive donor CD8 T cells migrate to secondary lymphoid tissues, where they proliferate and differentiate into anti-host effector T cells. In the late phase, alloactivated anti-host effector donor CD8 T cells recirculate and infiltrate into the peripheral tissues [7, 8]. It is probable that effector donor CD8 T cells, which infiltrate into the skin, liver, and intestine trigger GVHD, while those infiltrate into the tumor induce GVT effects. Therefore, selective inhibition of infiltration of effector donor CD8 T cells to the target tissues would reduce tissue specific GVHD without impairing GVT effects.

Lymphocyte trafficking is tightly regulated by the expression of particular adhesion molecules and chemokine receptors on the surface of lymphocytes, combined with the expression of ligands for these receptors by the target tissues [9–11]. It has become clear that several trafficking-associated molecules are actively involved in the development of GVHD [12, 13]. In the

early phase of allo-BMT, circulating naïve donor T cells rapidly enter into the host secondary lymphoid tissues through adhesion molecule L-selectin, $\alpha 4$ integrin, $\alpha 4\beta 7$, MAdCAM-1, and chemokine receptor CCR5, and preventive intervention of these molecules inhibit the development of anti-host CTL and ameliorate GVHD [14–16]. In the late phase, it has been reported that anti-host CTL infiltrate into liver via LFA-1-ICAM-1 interaction and CCR5-MIP-1α interaction and into the intestine via CXCR3–CXCR3 ligand interaction [17–20]. However, molecular interactions essential for the development of tissue-specific GVHD are not fully established, because severity of GVHD induced by CCR5$^{-/-}$ donor cells depends on the conditioning regimen [21], and GVHD to MHC is not reduced in recipients of CXCR3$^{-/-}$ donor cells [20]. These studies suggest that further spacio-temporal understanding of donor CD8 T cell dynamics is required for the separation of GVHD and GVT effects by targeting trafficking-associated molecule.

Intestinal GVHD is one of the most important complications arising with acute GVHD because the damaged intestinal epithelium allows spread of endotoxins into the systemic circulation, which amplifies subsequent systemic GVHD [22–25]. In this study, we first performed kinetic studies in a well-established graft-vs.-host reaction (GVHR) model to determine the trafficking-associated molecules involved in the intestinal infiltration of effector donor CD8 T cells during allogeneic reaction, and then explored whether inhibition of effector donor CD8 T cell infiltration into the intestine would segregate GVT effects from GVHR-associated intestinal injury.

MATERIALS AND METHODS

Mice and cell lines

C57BL/6 Ly5.2 (B6; CD45.2, H-2^b), (C57BL/6 x DBA/2) F1 (BDF1; CD45.2, H-2$^{b \times d}$) mice were purchased from CLEA Japan, Inc. (Tokyo, Japan). C57BL/6 Ly5.1 (CD45.1) was provided from Dr. Ishikawa (Keio University, Tokyo, Japan). All animal procedures described in this study were performed according to the guidelines for animal experiments of The University of Tokyo. P815 (H-2^d) and EL4 (H-2^b) cell lines were provided from Dr. Abe (Nipponkayaku, Tokyo, Japan). GFP-expressing tumorigenic P815 cell line was generated by retroviral transduction using pMY vector [26].

GVHD induction and tumor induction

For the GVHR model, 6 × 10^7 splenocytes from either B6 or BDF1 mice were injected intravenously into nonirradiated BDF1 mice on day 0. In GVT experiments in GVHR model, recipient mice were intravenously injected with 2 × 10^5 P815 or EL4 tumor cells on day −1. For the irradiated GVHD model, recipient mice received 13 Gy total body irradiation, split into two doses that were separated by 3 h on day −1. Bone marrow cells were prepared from the femurs and tibias of donor mice, followed by depletion of Ter-119 positive red blood cells and Thy1.2 positive mature T cells by MACS (Miltenyi Biotech, Bergisch Gladbach, Germany). Mature T cells were prepared from lymph nodes and spleen by negative selection with antibodies against CD11b, B220, and NK1.1 using MACS. The purity of selected T cells was at least 92%. Cell mixtures of 5 × 10^6 bone marrow cells supplemented with 5 × 10^6 T cells were then injected intravenously into irradiated recipient mice on day 0. In GVT experiments in irradiated GVHD model, recipient mice were intravenously injected with 1 × 10^4 P815 or EL4 tumor cells 2 h before transplantation.

Anti-mouse fractalkine monoclonal antibody

The anti-mouse fractalkine mAb was generated from Armenian hamsters immunized with recombinant mouse fractalkine by a standard method, and inhibited migration of mouse CX$_3$CR1-transfected B300.19 pre-B cells induced by mouse fractalkine (data not shown).

In vivo treatments

For the neutralizing experiments in GVHR model, 200 μg/100 μl PBS of anti-fractalkine mAb or 500 μg/ 100 μl PBS of anti-CXCL16 mAb [27] were administered i.p. into BDF1 mice on day 6, day 8, and day 10 or 100 μg/200 μl PBS of anti-MAdCAM-1 mAb (MECA367, BD PharMingen, San Diego, CA) was administered i.p. on day 7 after GVHR induction. Normal hamster IgG or rat IgG was used as a control antibody. In the GVHD model, the same dose of anti-fractalkine mAb and anti-CXCL16 mAb were administrated every 4 days and anti-MAdCAM-1 mAb was administrated every 7 days from day 4 to day 32 after GVHD induction.

Cell preparation, antibodies, flow cytometry, and cell sorting

Intestinal and hepatic mononuclear cells were isolated according to the methods described previously [28, 18]. In brief, the small intestine was removed and Peyer's patches were excised from the intestine. The inverted intestine was then cut into four segments, and the segments were transferred to a 50 ml conical tube containing 45 ml RPMI-1640, 5% FBS, 25 mM HEPES. The tube was shaken at 37°C for 45 min. For the preparation of intestinal intraepithelial lymphocytes (IEL), cell suspensions were collected and passed through a nylon-wool column to deplete cell debris and sticky cells. Subsequently, the cells were subjected to 44/70% Percoll (Sigma-Aldrich, St. Louis, MO) gradient, and IEL were recovered at the interphase. For the preparation of lamina propria lymphocytes (LPL), residual intestinal pieces were digested with 50 U/ml collagenase (Type VIII, Sigma-Aldrich), and supernatants were subjected to percoll density gradient as described above. We mainly examined the IEL compartment as intestine-infiltrating lymphocytes, because the epithelium is the major target of intestinal GVHD. LPL compartment was only used in chemotaxis assay. For the preparation of hepatic lymphocytes, livers were perfused with PBS and pressed through stainless-steel mesh and suspended in 5% FBS-DMEM. The cell suspensions were treated with 33% Percoll containing 100 U/ml heparin and were centrifuged at 800 g for 10 min at room temperature. The pellets were resuspended in ACK lysing buffer, washed 2 times in DMEM, and resuspended in 10% FBS-DMEM. The mAbs specific for mouse FcγR (2.4G2), CD8 (53-6.7), CD45.1 (A20), CD62L (MEL-14), and α4β7 (DATK32) were purchased from BD PharMingen, and anti-mouse CCR9 mAb were purchased from R&D Systems (Minneapolis, MN). After incubation with anti-mouse FcγR mAb, cells were stained with appropriate concentrations of mAbs and then analyzed by EPICS ELITE ESP cell sorter (Beckman Coulter, Hialeah, FL) with EXPO32 software. Dead cells were excluded on the basis of forward and sidescatter profiles, and propidium iodide staining. Donor CD8 T cells were purified by cell sorting, and the sorted cells showed >98% purity. For IFN-γ detection, cells were stimulated with 5 ng/ml PMA and 0.5 μg/ml ionomycin for 5 h in the presence of 10 μg/ml brefeldin A followed by intracellular staining using Cytofix/Cytoperm Kit (BD PharMingen), according to the manufacturer's directions.

Chemotaxis assay

Chemotaxis assay was performed with ChemoTx plate (Neuro Probe, Gaithersburg, MD), according to the manufacturer's instructions. In brief, untreated CD8 T cells from B6 spleen or intestine, infiltrating donor CD8 T cells from GVHD induced BDF1 mice were suspended at 2 × 10^6 cells/ml in RPMI 1640 containing 0.5% BSA and 20 mM HEPES. Twenty-five microliters of cell suspensions were loaded on the membrane plate and placed onto a flat-bottomed 96-well microtiter plate containing 29 μl of fractalkine (10^{-8} M), TECK (10^{-7} M), and SLC (10^{-8} M).

Immunofluorescence staining and TUNEL assay

Recipient mice of GFP-expressing P815 were perfused with 4% paraformaldehyde/PBS. Immunofluorescent staining of fresh or paraformaldehyde fixed frozen sections were performed as described previously [29]. In brief, cryosections were fixed in ice-cold acetone and were preincubated with Block Ace (Dainippon Pharmaceutical Co. Ltd, Tokyo, Japan). Subsequently, samples were incubated with primary antibodies or appropriate control antibodies, followed by incubation with Alexa-dye labeled appropriate secondary reagents

(Invitrogen Japan K. K., Tokyo, Japan). Anti-smooth muscle actin mAb (clone 1A4), Anti-EpCAM mAb (clone G8.8), and ER-TR7 were purchased from Sigma-Aldrich (St. Louis, MO, USA). BD PharMingen and BMA Biomedicals (Augst, Switzerland), respectively. Anti-fractalkine pAb and anti-CXCL16 pAb were purchased from R&D Systems. The sections were analyzed by an Olympus IX-70 confocal laser-scanning microscope system (Olympus Optical, Tokyo, Japan). For the detection apoptotic cell death, horizontal sections of intestine were stained with in situ cell death detection POD kit (Roche, Mannheim, Germany), according to the manufacturer's instruction. For the counts of apoptotic cells in the intestine, 10 fields (330 µm×330 µm) of horizontal sections were examined for each mice, and the average number of TUNEL-positive cells/field of three mice was calculated.

Real-time RT-PCR analysis

Real-time RT-PCR was performed as described previously with a set of primers and Taqman probes corresponding to CCR1, CCR2, CCR5, CCR7, CCR9, CXCR3, and GAPDH, as described previously [29]. The sense primer for CXCR6 was 5'-AAGCTGACGACTCTGACAGATGTGT-3', the antisense primer was 5'-CCAAAAGGGCAGAGTACAGACAA-3', the probe was 5'-CTGCTGAACTTGCCC CTGGCTGAC-3'. The sense primer for CX_3CR1 was 5'- CCGCCAACTCCATGAACAA-3', the antisense primer was 5'-CGTCTG-GATGATGCGGAAGTA-3', the probe was 5'-CGTCACCCCAGTTCATGT-TCACAAATAG-3'. PCR was run in triplicate for each primer/template set, and the quantity of target mRNA was normalized by the level of GAPDH in each sample.

Short-term migration assay

Mononuclear cells were collected from either spleen of normal B6 mice (untreated) or peripheral blood of GVHR-induced BDF1 mice on day 10 (allo-activated), and CD8 T cells were negatively enriched by MACS with antibody against CD11b, B220, NK1.1, CD4, and CD45.2 (The purity of CD45.1$^+$ CD8$^+$ cells >90%). Untreated or allo-activated donor CD8 T cells were then labeled with CFSE and transferred into normal BDF1 mice (3×10^6 cells/mice). Two hours later, mice were perfused with 50 ml of PBS, and vertical sections of small intestine were embedded in Tissue-Teck OCT compound. Twelve-micrometer frozen sections of small intestine were analyzed by AX80 fluorescent microscopy (Olympus Optical). For the evaluation of trafficking efficiency to the intestine, 100 arbitrary villi/representative sections that exhibited exactly the vertical profile were chosen, and the numbers of CFSE-positive cells were counted.

Cytotoxicity assay

Donor CD8 T cells were purified from spleen of normal B6 or liver of GVHR-induced mice treated with control- or anti-fractalkine- or anti-MAdCAM-1 antibody. Effector (E) donor CD8 T cells were incubated with 1 × 10^4 target (T) P815 or EL4 cells for 5 h at 37°C. In all cases, the starting E:T ratio was adjusted to obtain an identical ratio of donor CD8 T cells to target cells. Effectors were tested in triplicate at four E:T ratios. After the incubation, cytotoxicity against target cells was determined by LDH cytotoxicity detection kit (Takara Biomedicals, Tokyo, Japan). The percent-specific LDH release was calculated from (experimental release–spontaneous release)/(detergent release–spontaneous release) ×100.

Biochemical analysis

The increase in serum alanine transferase (ALT) concentration, which is an indicator of liver damage, was determined with a Fuji DRY-CHEM 5500V (Fuji Medical Systems, Tokyo, Japan).

Statistical analysis

Statistical comparisons between groups were evaluated using the Student's t-test, except for survival data. Data were presented as means with 95% confidence intervals (CIs). Differences in survival among groups of mice were evaluated with a log-rank test of the Kaplan-Meier survival curves. $P < 0.05$ was considered to be statistically significant.

RESULTS

Development of effector donor CD8 T cells and intestinal injury during GVHR

Infiltration of anti-host CTL into intestine is thought to be a trigger of intestinal injury in GVHD. To confirm this notion, we first performed the kinetic studies in GVHR model, in which intestinal injury is mediated solely by allogeneic reaction. The number of donor CD8 T cells in the spleen and mesenteric lymph nodes (MLN) increased from day 2 after GVHR induction, peaked on day 10, then decreased thereafter. Unlike secondary lymphoid tissues, in the small intestine, donor CD8 T cells were rarely detected during the first 8 days and rapidly increased from day 8 to day 14 with CD11a^{hi} CD44^{hi} IFN-γ producing effector cell phenotype (**Fig. 1A–C**). Immunohistological analysis revealed that donor CD8 T cells were barely detectable in the intestine during the first 6 days of GVHR, but they rapidly infiltrated the lamina propria, which located adjacent to crypt epithelium with only a few in the villous epithelium on day 8 (Fig. 1D). Crypt cell apoptosis is a typical feature of intestinal GVHD [30]. Consistent with the kinetics of intestine infiltrating effector donor CD8 T cells, TUNEL-positive apoptotic crypt epithelial cells were rarely detected before day 6; however, they rapidly increased by day 8 and remained high over the following days (Fig. 1E, F). These results suggest that the infiltration of effector donor CD8 T cells into the intestine, which take place during the late phase of GVHR (i.e., days 8-14), is closely associated with the development of intestinal injury.

Developmental changes of trafficking property of donor CD8 T cells during GVHR

It is well established that the migration properties of T cells critically depend on their differentiation state. On the basis of this concept, we hypothesized that intestinal infiltration of donor CD8 T cells in the late phase is induced by developmental changes of trafficking property of donor CD8 T cells during GVHR. To compare migration properties of primary circulating donor CD8 T cells (i.e., untreated donor CD8 T cells) and allo-activated recirculating donor CD8 T cells (i.e., donor CD8 T cells recovered from peripheral blood of GVHR induced mice on day 10), we performed the short-term migration assay. Two hours after adoptive transfer, untreated donor CD8 T cells preferentially migrated into host lymphoid tissues, including lymph nodes, spleen, and Peyer's patches but did not migrate to the intestinal lamina propria. In contrast, allo-activated donor CD8 T cells preferentially migrated into non-lymphoid tissues, including intestine and liver, but did not migrate to lymphoid tissues (**Fig. 2A, B** and data not shown). The migration of lymphocytes to intestinal nonlymphoid compartment is highly dependent on the expression of intestinal homing receptor α4β7 [31]. Thus, we next analyzed the kinetics of α4β7 expression on donor CD8 T cells to examine whether the expression of α4β7 correlate with intestinal homing property. Allo-activated donor CD8 T cells migrate from secondary lymphoid tissues to the intestine via peripheral blood. During the first 5 days of GVHR, most of the circulating peripheral blood donor CD8 T cells expressed high levels of
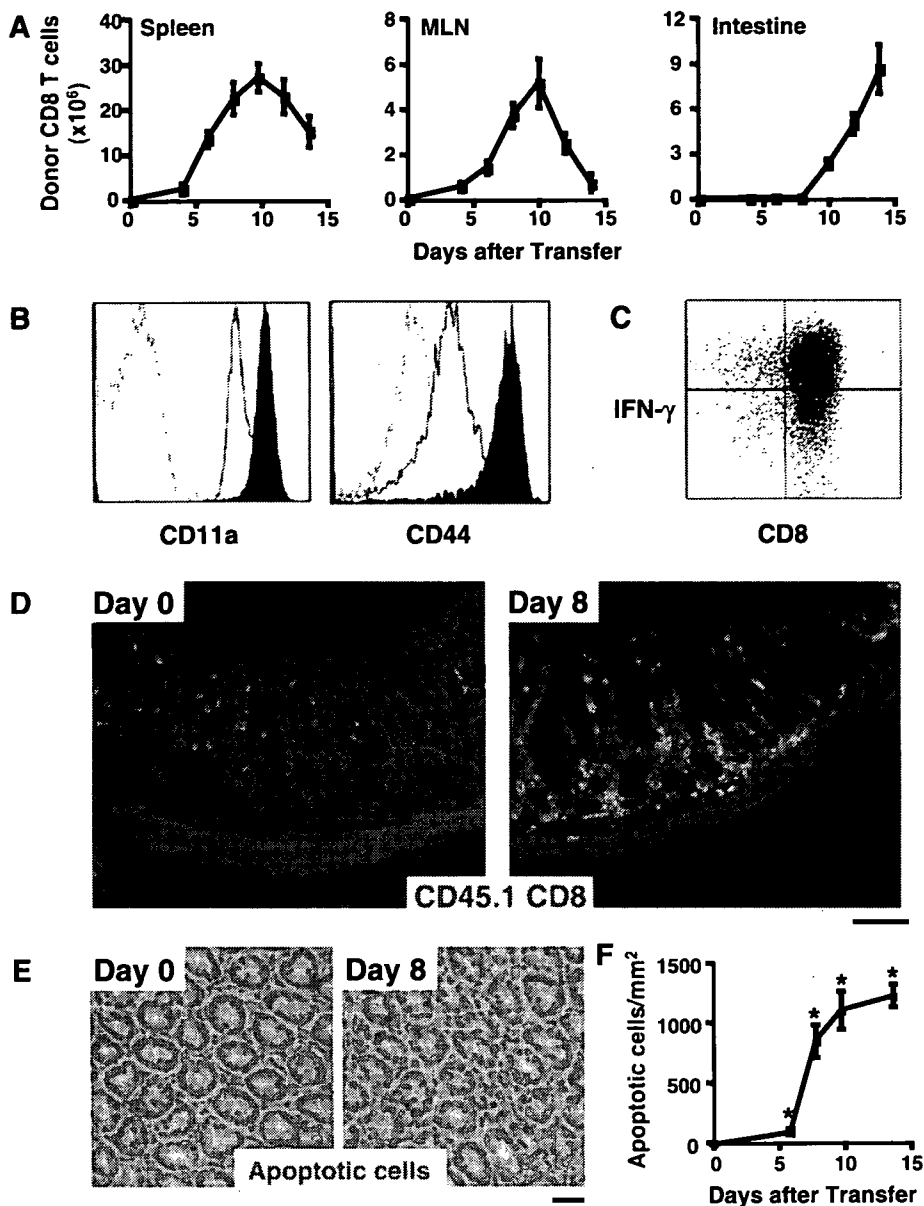
Fig. 1. Kinetics of donor CD8 T cells and development of intestinal injury during GVHR. CD45.2$^+$ recipient BDF1 mice were inoculated with CD45.1$^+$ B6 donor splenocytes. (A) Absolute number of donor CD8 T cells in the spleen, mesenteric lymph nodes (MLN), and intestine were analyzed by flow cytometry at several time points post-GVHR induction. Mean values with 95% confidence intervals (n=6 mice/time points, pooled data from two independent experiments). Cell surface markers (B) and IFN-g production (C) of intestine-infiltrating donor CD8 T cells on day 10. Dotted histogram indicates background staining with isotype control, open histogram indicates untreated donor CD8 T cells, and solid histogram indicates intestine-infiltrating donor CD8 T cells. The number in the quadrant represents the percentage of IFN-γ^+ cells/donor CD8 T cells after in vitro stimulation (unstimulated control were <1%). (D) Vertical sections of small intestine were prepared on day 0 and day 8 and costained with anti-CD45.1 Ab (green) and anti-CD8 Ab (red). (E) Horizontal sections of intestine were prepared on day 0 and day 8, and apoptotic cells in the crypt epithelium were detected by TUNEL reaction. Apoptotic cells are shown in brown, and mononuclear cells are counterstained with hematoxylin (blue). Scale bars: 50 μm (B), 25 μm (C). Reproducible results were obtained from two independent similar analyses. (F) Crypt cell apoptosis was quantified as described in Materials and Methods. Data are expressed as the number of TUNEL-positive cells in crypt area (/mm^2). Mean values with 95% confidence intervals (10 fields/mice, n=6 mice/time points, pooled data from 2 independent experiments). *, $P < 0.001$ vs. day 0.

CD62L, a homing receptor for the peripheral lymph nodes [32], whereas only a minority of these cells expressed α4β7. The ratio of CD62L^{hi} cells among the circulating donor CD8 T cells gradually decreased with concurrent increase of α4β7$^+$ cells from day 5 to day 9. In addition, the majority of the intestine-infiltrating donor CD8 T cells also expressed α4β7 (Fig. 2C).

We next analyzed the relative chemokine receptor expression in allo-activated donor CD8 T cells to untreated donor CD8 T cells, because chemokine receptor expression closely associated with the intestinal homing property. Real-time PCR analysis revealed that untreated donor CD8 T cells expressed high levels of mRNA for the chemokine receptor CCR7, CCR9, and relatively low levels of those for CCR1, CCR2, CCR5, CXCR3, CXCR6, and CX$_3$CR1. In contrast, donor CD8 T cells isolated from GVHR-induced intestine on day 10 of GVHR showed down-regulated expression of CCR7 and CCR9, but

up-regulated expression of CXCR6 and CX$_3$CR1 (Fig. 2D). The down-regulation of CCR9, one of the intestinal homing receptor, and up-regulation of CX$_3$CR1 were confirmed by flow cytometry and chemotaxis assay to TECK or fractalkine (Fig. 2E, F). Lymphocyte migration requires the expression of ligands for homing receptors by target tissues. To examine the expression of MAdCAM-1 (α4β7 ligand [33]), CXCL16 (CXCR6 ligand [34]), and fractalkine/CX$_3$CL1 (CX$_3$CR1 ligand [35]), we performed the immunohistological analysis. CXCL16 has been reported to be expressed on dendritic cells, macrophages, smooth muscle cells and splenic red pulp [34, 36, 37], but its distribution in intestine has not been established. Therefore, we first examined the CXCL16 expression in the normal intestine. As shown in Fig. 2G, CXCL16 was expressed on the smooth muscle actin-positive smooth muscle cells in the lamina muscularis mucosa and the muscular coat of normal

Ueha et al. Migration of donor CD8 T cells during intestinal GVHR   179

−82−

intestine. CXCL16 expression was also detected in a part of smooth muscle actin negative cells but was not detected on tomato-lectin labeled vascular endothelium (Fig. 2G). The expression of CXCL16 in intestine was not changed during GVHR (Fig. 2H). MAdCAM-1 is constitutively expressed on a part of the endothelium in the intestinal lamina propria, known as the lamina propria venules, and donor cells were located within or adjacent to the MAdCAM-1^{+} lamina propria venules on day 7 of GVHR (Fig. 2H). It has been reported that fractalkine is expressed on intestinal epithelial cells [38, 39]. Consistent with previous reports, fractalkine was detected on the intestinal epithelium, with the villous epithelial cells more strongly stained than the crypt epithelial cells (Fig. 2H). The

expression of MAdCAM-1, CXCL16, and fractalkine remained almost constant during GVHR in both mRNA and protein level (data not shown). Importantly, we could not detect the protein expression of MAdCAM-1 and fractalkine in the liver during GVHR (data not shown).

Anti-fractalkine or anti-MAdCAM-1 antibodies selectively inhibit intestinal infiltration of effector donor CD8 T cells and reduce intestinal injury

The up-regulation of α4β7, CXCR6, and CX$_3$CR1 in effector donor CD8 T cells suggest that α4β7-MAdCAM-1, CXCR6-CXCL16, and CX$_3$CR1-fractalkine interactions are involved in the recruitment of effector donor CD8 T cells to intestine and
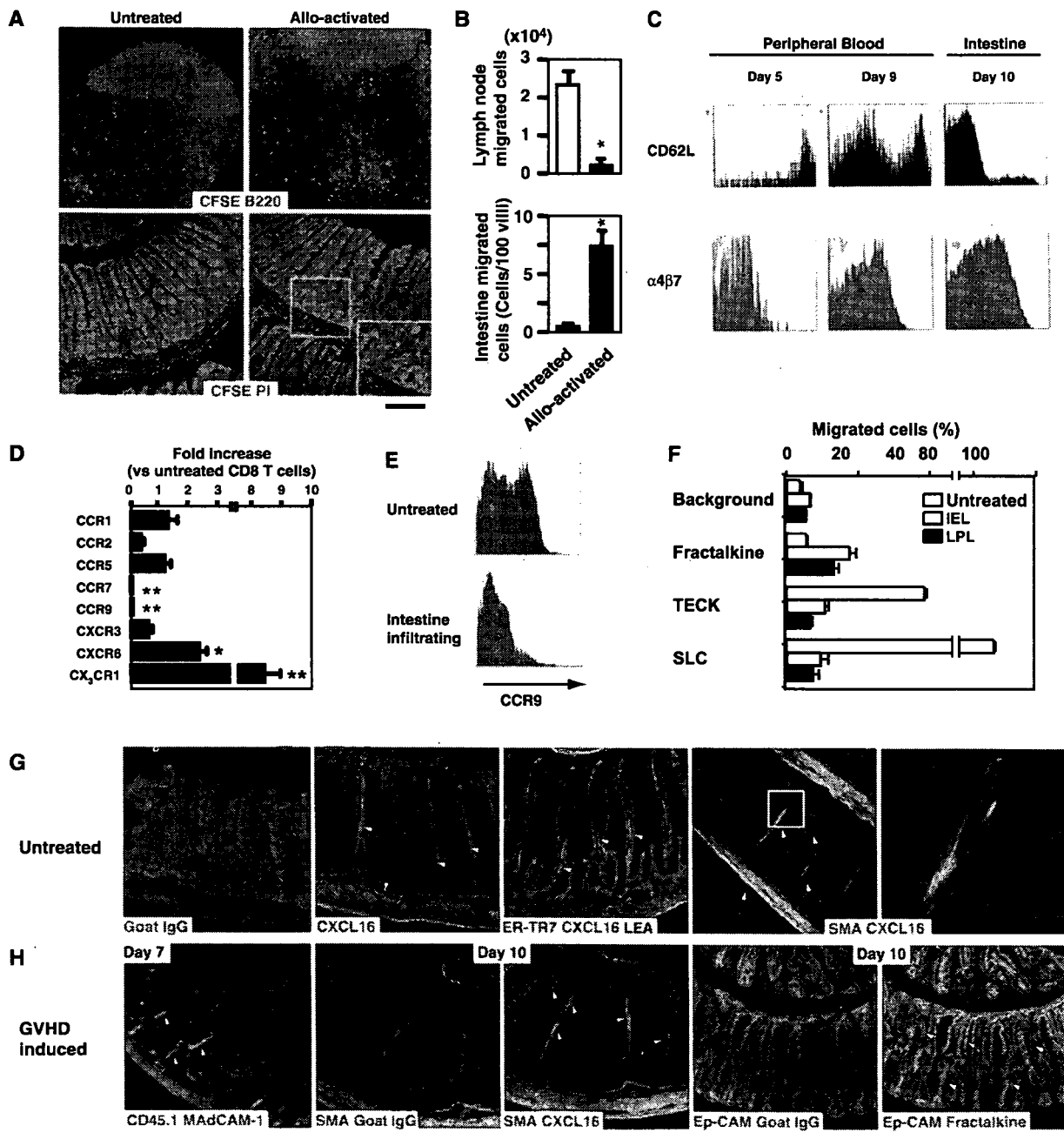
promote the intestinal injury. To test this, we administered neutralizing antibodies against MAdCAM-1, CXCL16, and fractalkine to GVHR-induced mice. In the neutralization experiments, we administered antibodies after the expansion of donor CD8 T cells to exclude the effects on the development of effector cells in the early phase [16]. As shown in **Fig. 3**, administration of anti-fractalkine Ab significantly decreased the number of donor CD8 T cells in the intestine by 61% ($P=0.001$) and reduced the number of apoptotic crypt cells by 43% ($P<0.001$) compared with control antibody-treated group, whereas it had no significant effects on the number of donor CD8 T cells in the liver or serum ALT levels. Administration of anti-MAdCAM-1 Ab also decreased the number of donor CD8 T cells in the intestine by 85% ($P<0.001$) and reduced the number of apoptotic cells by 75% ($P<0.001$), whereas we did not see any significant changes in the liver. Treatment with anti-CXCL16 Ab decreased the number of CXCR6 positive donor CD8 T cells in the liver (30-35% of donor CD8 T cells in the liver of GVHR-induced mice on day 14, data not shown) but did not significantly affect overall pathology of intestinal- or liver-GVHR (data not shown).

Anti-fractalkine Ab or anti-MAdCAM-1 Ab treatments preserve GVT effects

We previously demonstrated that pretreatment of recipient mice with anti-MAdCAM-1 Ab inhibits the development of anti-host CTL activity during GVHR [16]. Preservation of the anti-host CTL activity is necessary for optimal GVT effects. Therefore, we examined the effects of the anti-fractalkine Ab or anti-MAdCAM-1 Ab treatments on the development of anti-host CTL activity. As shown in **Fig. 4A**, untreated donor CD8 T cells from normal B6 spleen showed only background lysis against Host-type P815 cells, whereas liver-infiltrating allo-activated donor CD8 T cells from day 14 after GVHR induction showed specific lysis against P815 but only background lysis against donor-type EL4 leukemia cells. Liver-infiltrating allo-activated donor CD8 T cells from anti-fractalkine antibody- or anti-MAdCAM-1 antibody-treated groups

exhibited comparable lysis against P815 to those from the control antibody-treated group, suggesting that anti-fractalkine and anti-MAdCAM-1 antibody treatment does not impair the induction of anti-host CTL activity in our protocol. Next, we examined the effects of the antibody treatments on the infiltration of allo-activated donor CD8 T cells to hepatic tumor. As shown in Fig. 4B, GVHR-induced mice with GFP-expressing P815 tumor cells and control antibody treatment showed massive infiltration by donor CD8 T cells in the hepatic tumor on day 10 of GVHR. The extent of donor CD8 T cell infiltration was similar in the recipient mice treated with anti-MAdCAM-1 Ab or anti-fractalkine Ab (data not shown). To examine the mechanisms of the segregation of GVT effects and GVHD by the antibody treatments, we analyzed the expression of fractalkine and MAdCAM-1 in the GVHR-induced liver with hepatic tumor. As shown in Fig. 4C, fractalkine and MAdCAM-1 mRNA expression in the liver is relatively low compare with that of intestine. Furthermore, we could not detect the expression of MAdCAM-1 and fractalkine in tumor vasculature by immunohistological analysis (data not shown). These results suggest that administration of anti-fractalkine Ab or anti-MAdCAM-1 Ab after the expansion of donor CD8 T cells preserves induction of anti-host CTL activity and infiltration of CTL in the hepatic tumor.

Anti-fractalkine Ab or anti-MAdCAM-1 Ab treatments reduce severity and mortality of GVHD without affecting GVT-associated survival advantage

We finally addressed the clinical applicability of anti-fractalkine or anti-MAdCAM-1 antibody treatments using a GVHD model with myeloablative conditioning. Lethally irradiated recipient mice of allogeneic bone marrow and T cells were treated with control Ab or anti-fractalkine Ab or anti-MAdCAM-1 Ab as described in Materials and Methods. As shown in **Fig. 5A**, administration of anti-fractalkine Ab or anti-MAdCAM-1 Ab exhibited a significant survival advantage and reduced body weight loss compared with control antibody-

---

Fig. 2. Changes in the trafficking properties of donor CD8 T cells and expression of trafficking-associated molecules during acute GVHR. (A) In vivo migration of untreated- or allo-activated donor CD8 T cells. CFSE-labeled donor CD8 T cells from normal B6 mice (untreated) or peripheral blood of GVHR-induced mice (allo-activated) were transferred into untreated BDF1 mice. Two hours after transfer. CFSE-positive cells in the lymph nodes and intestine were analyzed by a confocal laser-scanning microscopy. Scale Bar: 50 μm. Representative images from three independent experiments are shown. (B) Migration of untreated or allo-activated donor CD8 T cells to lymph nodes and intestine of untreated BDF1 mice were quantified by flow cytometry or confocal laser-scanning microscopy, respectively. Migration efficiency to intestine are shown in the number of CFSE-positive cells/100 villi. Mean values with 95% confidence intervals ($n=3$ mice/groups). *. $P < 0.001$. (C) Expression of CD62L and α4β7 on circulating or intestine-infiltrating donor CD8 T cells. Open histogram in the lower panel indicates background staining with isotype control. Representative profiles of three mice are shown. (D) Levels of chemokine receptor mRNA in the intestine-infiltrating donor CD8 T cells on day 10. Data are shown in fold increase relative to CD8 T cells from normal B6 mice. Mean values with 95% confidence intervals ($n=3$ mice/groups, representative data from two independent experiments). *. $P = 0.046$. **. $P < 0.001$ vs. CD8 T cells from normal B6 mice. (E) CCR9 expression on untreated- and intestine infiltrating-donor CD8 T cells was analyzed by flow cytometry. Open histogram indicates background staining with isotype control. (F) Untreated donor CD8 T cells were prepared from normal B6 spleen, and intestine-infiltrating lymphocytes were prepared from intestinal intraepithelial lymphocyte compartment (IEL) and lamina propria lymphocyte compartment (LPL) of GVHR-induced mice on day 10. Chemotaxis response of untreated and intestine-infiltrating donor CD8 T cells to fractalkine (10^{-8} M). TECK (10^{-7} M), and SLC (10^{-8} M) were evaluated using a Boyden chamber. Data represent the percentage of migrated cells of triplicates. Representative data from two independent experiments. *. $P = 0.049$. **. $P < 0.001$ vs. background. (G) Vertical section of small intestine was prepared from normal BDF1 mice and stained with control goat IgG or anti-CXCL16 Ab (Red). Costaining with anti-smooth muscle actin (SMA) Ab indicates smooth muscle cells and ER-TR7 (green) indicates reticular fibroblast or reticular fiber. Some mice were injected intravenously with fluorescein-conjugated tomato lectin (LEA) before sacrifice to identify luminal surface of vascular endothelium (blue). Arrows indicate specific signal of CXCL16. (H) Vertical sections of intestine were prepared from GVHR-induced mice on day 7 or day 10. Day 7 section was costained with anti-MAdCAM-1 Ab (red) and anti-CD45.1 Ab (green). Day 10 sections were stained with control goat IgG or anti-CXCL16 Ab or anti-fractalkine Ab (Red). Costaining with anti-SMA Ab or anti-EpCAM Ab (green) indicates smooth muscle cells or epithelial cells, respectively. Scale bars: 50 μm. Arrows indicate specific signal of MAdCAM-1 (left). CXCL16 (center). and fractalkine (right). respectively. Representative image from 3 independent experiments are shown.
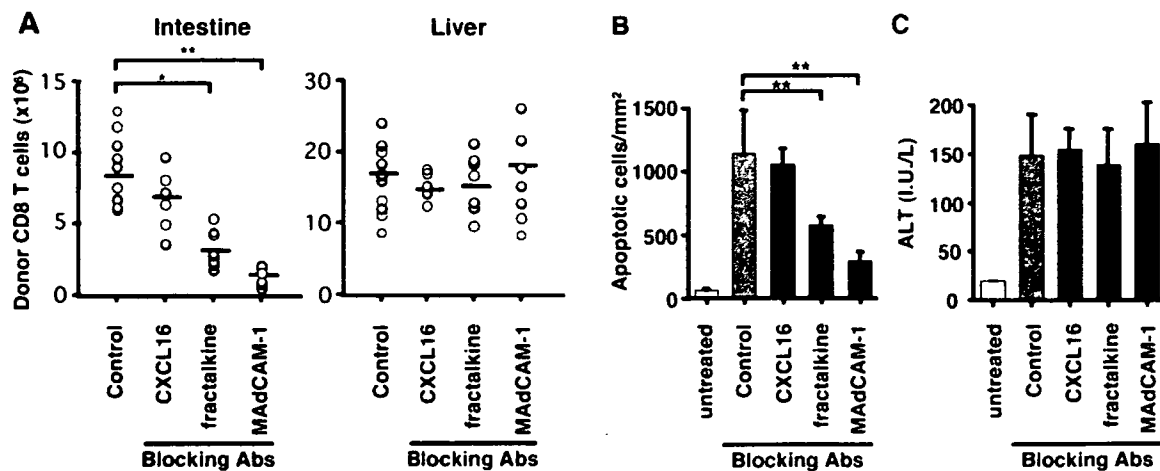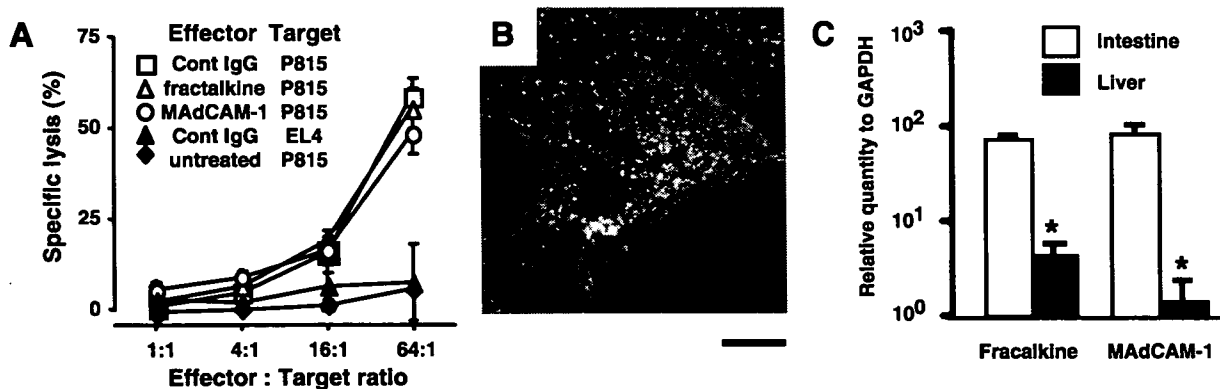
Fig. 3. Anti-fractalkine or anti-MAdCAM-1 antibodies selectively inhibit intestinal infiltration of donor CD8 T cells and reduce intestinal injury. Anti-fractalkine Ab or anti-CXCL16 Ab were administered i.p. into BDF1 mice on day 6, day 8, and day 10, or anti-MAdCAM-1 Ab was administered i.p. on day 7 of GVHR. Normal hamster IgG or rat IgG was used as control antibody. (A) The number of intestine- and liver- infiltrating donor CD8 T cells on day 14. The horizontal lines mark the mean value. The number of crypt epithelial cell apoptosis (B) and serum ALT levels (C) on day 14. Mean values with 95% confidence intervals (n>6, pooled data of 3 independent experiments. *, P=0.001. **, P<0.001 vs. control).

treated group (Survival: P<0.001 and P=0.004 compared with control antibody-treated group, respectively. Body weight loss: P<0.05 (days 10–20) and P<0.05 (days 10–20) compared with control antibody-treated group, respectively). In the GVT experiments, recipient mice of syngeneic BMT and P815 died from tumor infiltration in the liver by day 18 (median survival=16.6, n=10), whereas recipients of allogeneic BMT and P815 with control antibodies died from GVHD, identified by the absence of tumor nodules in the liver, by day 34 (median survival=27.4 and 27.0, P<0.001 and P<0.001, n=10, respectively), suggesting a GVT-associated survival advantage. Allogeneic recipients treated with antifractalkine Ab or anti-MAdCAM-1 Ab also died from GVHD but exhibited significant
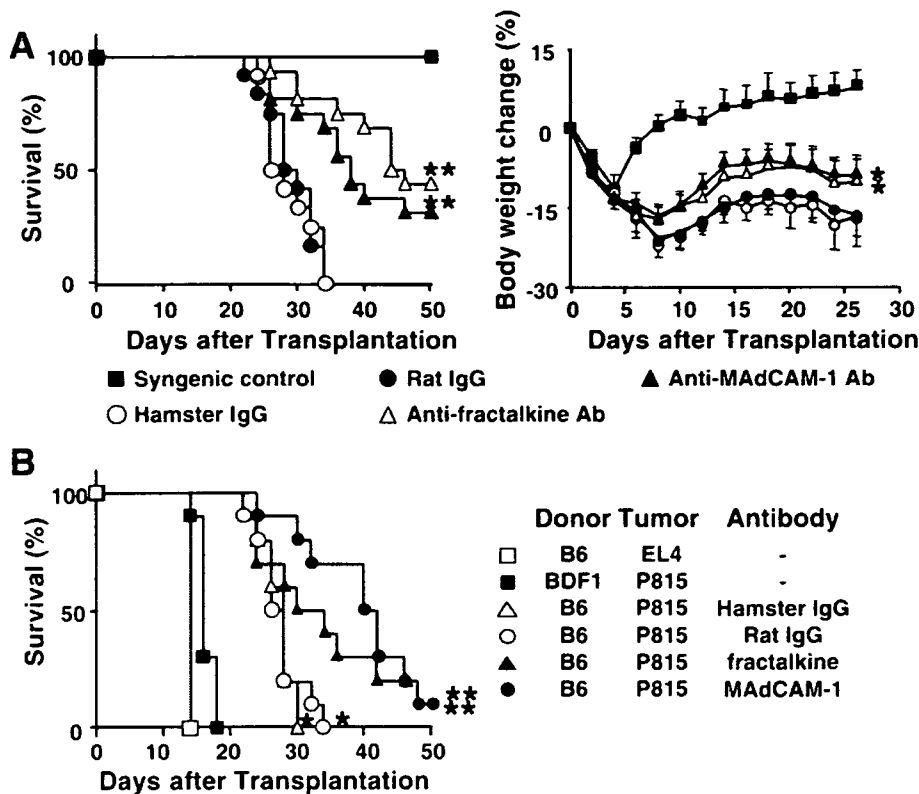
survival advantage (P<0.001 and P<0.001 compared with control antibody-treated groups, respectively), suggesting a preservation of GVT effects (Fig. 5B). Taken together, these results suggest that intervention of α4β7-MAdCAM-1 and CX3CR1-fractalkine interactions selectively inhibits intestinal infiltration of effector donor CD8 T cells, which results in the alleviation of GVHD without impairing GVT effects.

DISCUSSION

It is widely accepted that myeloablative conditioning in BMT is closely associated with the severity of GVHD. However, my-

Fig. 4. Anti-fractalkine or anti-MAdCAM-1 antibodies preserve GVT effects. (A) Anti-P815 (H-2^d) CTL activity of liver-infiltrating donor CD8 T cells from control antibody- (open squares) or anti-fractalkine Ab- (open triangles) or anti-MAdCAM-1 Ab- (open circles) treated GVHR-induced mice on day 10. Anti-EL4 (H-2^b) CTL activity of those from control Ab-treated group (closed triangles) and anti-P815 (H-2^d) CTL activity of CD8 T cells from B6 mice (closed diamonds) indicate background lysis. Mean values with 95% confidence intervals of three mice. Representative data of two independent experiments. (B) Infiltration of donor CD8 T cells in the tumor site. GVHR-induced mice were inoculated with GFP-expressing P815 on day −1. Tumor-infiltrating liver sections were stained with anti-CD45.1 Ab (red) and anti-CD8 Ab (blue). GFP-bearing P815 was shown in green. Scale bars: 50 μm. Representative images from three independent experiments are shown. (C) Fractalkine and MAdCAM-1 mRNA expression in the intestine and liver of GVHR-induced mice bearing hepatic tumor were analyzed by real-time PCR. Mean values with 95% confidence intervals (n=6. pooled data of 2 independent experiments) . *, P < 0.01.

A

Survival (%) vs Days after Transplantation (0-50)
Body weight change (%) vs Days after Transplantation (0-30)

■ Syngenic control ● Rat IgG ▲ Anti-MAdCAM-1 Ab
○ Hamster IgG △ Anti-fractalkine Ab

B

Survival (%) vs Days after Transplantation (0-50)

	Donor	Tumor	Antibody
□	B6	EL4	-
■	BDF1	P815	-
△	B6	P815	Hamster IgG
○	B6	P815	Rat IgG
▲	B6	P815	fractalkine
●	B6	P815	MAdCAM-1

Fig. 5. Anti-fractalkine or anti-MAdCAM-1 antibodies alleviate GVHD without impairing GVT effects. Lethally irradiated recipients received syngeneic ($n=10$, solid squares) or allogeneic BMT. Recipients of allogeneic BMT were treated with anti-fractalkine Ab ($n=16$, open triangles) or hamster IgG ($n=12$, open circles) every 4 days. or anti-MAdCAM-1 Ab ($n=16$, solid triangles) or rat IgG ($n=12$, solid circles) every 7 days from day 4 to day 32 after BMT. (A) Survival and body weight change. Body weight changes are shown in mean values with 95% confidence intervals. Results represent pooled data of 2 independent experiments. *. $P < 0.05$ vs. control antibody-treated groups, from day 10 to day 20. **. $P < 0.001$ vs. control antibody-treated groups. (B) Lethally irradiated recipients received syngeneic or allogeneic BMT with tumor cells and antibody treatments. Survival in the recipients of P815 and allogeneic donor cells with hamster IgG- (open triangles), rat IgG- (open circles). anti-MAdCAM-1 Ab- (solid circles), anti-fractalkine Ab- (solid triangles) treatment, recipients of P815 and syngenic donor cells (solid squares), recipients of EL4 and allogeneic donor cells (open squares). $n = 10$ mice/group, pooled data of two independent experiments. *, $P < 0.001$ vs. recipients of P815 and syngenic BMT. **, $P < 0.001$ vs. control antibody treated groups.

eloablative conditioning in animal models hinders the understanding of allo-specific immune response, as systemic irradiation induces systemic inflammation and lymphopenia, which drives antigen-nonspecific homeostatic proliferation of donor T cells [40]. Using a well-established GVHR model, we demonstrated that allo-reactive donor CD8 T cells redistribute from secondary lymphoid tissues to the peripheral target tissues during GVHR, as they differentiate into the effector cells. Also, intestinal infiltration of effector donor CD8 T cells was closely associated with the crypt epithelial cell apoptosis. Our results from nonirradiated GVHR model suggest that the infiltration of donor CD8 T cells not only amplifies but also triggers the intestinal injury during GVHD.

During GVHR, circulating donor CD8 T cells gradually up-regulate the adhesion molecule $\alpha4\beta7$ as they differentiate into effector cells. $\alpha4\beta7$ is an important intestinal homing receptor for both the naive and effector/memory T cells, and $\alpha4\beta7$-expressing lymphocytes interact with MAdCAM-1-bearing high endothelial venules in Peyer's patches and MLN, as well as with the lamina propria venules in the intestinal lamina propria [31, 33]. We previously demonstrated that administration of neutralizing antibody against MAdCAM-1 before GVHR induction successfully inhibits the migration of donor CD8 T cells to Peyer's patches and prevents induction of anti-host CTL [16]. Petrovic et al. reported that $\alpha4\beta7^-$ donor T cells induced less GVHD morbidity and mortality compared with $\alpha4\beta7^+$ donor T cells [15]. However, segregation of GVT effects and intestinal GVHD by preventive intervention of $\alpha4\beta7$-MAdCAM-1 interaction is thought to be difficult, because $\alpha4\beta7$-MAdCAM-1 interaction is required for the induction of

anti-host/tumor CTL and $\alpha4\beta7^-$ naïve CD8 T cells can differentiate into $\alpha4\beta7^+$ effector CD8 T cells. Our data demonstrate that the administration of anti-MAdCAM-1 Ab, even after the expansion of allo-reactive donor CD8 T cells, selectively reduced the numbers of intestine-infiltrating donor CD8 T cells without affecting induction of anti-host/tumor CTL. Thus, we suggest that therapeutic intervention of $\alpha4\beta7$-MAdCAM-1 interaction may be effective for the segregation of GVT effects from intestinal injury.

In addition to $\alpha4\beta7$, intestine-infiltrating donor CD8 T cells up-regulated the chemokine receptor CXCR6 and CX_3CR1. It has been reported that CX_3CR1 is expressed on terminally differentiated effector CD8 T cells [41]. Consistent with the previous reports, intestine-infiltrating donor CD8 T cells exhibited typical effector T cell phenotype. In general, chemokine/chemokine receptor interaction induces the firm adhesion of lymphocytes to endothelial cells and extravasation of lymphocyte into the tissues. However, we could not detect the expression of fractalkine on the intestinal endothelium. Among the chemokine family, fractalkine has unique structural and functional features, as it is expressed on the cell surface where it acts as an adhesion molecule, and when soluble fractalkine is released from the cell surface by proteolysis, it can act as a chemoattractant [35]. So, the possible role of fractalkine-CX_3CR1 is that soluble fractalkine may be released from the epithelial cells and recruit CX_3CR1-positive effector cells to the epithelial cells, while transmembrane fractalkine expressed on the epithelial cells may promote the firm adhesion between CX_3CR1-positive effector cells and epithelial cells and, through this interaction, enhance the retention of effector

Ueha et al. **Migration of donor CD8 T cells during intestinal GVHR   183**

donor CD8 T cells in epithelium and the contact-dependent cytotoxic pathway. Also, Niess et al. reported that CX$_3$CR1-fractalkine interaction is important for intestinal DCs to sample luminal antigens [42]. Therefore, CX$_3$CR1-fractalkine interaction may promote the induction of allo-MHC restricted luminal antigen-specific donor CD8 T cells in draining lymph nodes and/or induce activation of intestine infiltrating donor CD8 T cells through host-derived luminal antigen-bearing intestinal DCs. In addition, CX$_3$CR1-fractalkine interaction has been reported to be involved in cell survival and T cell costimulation [43, 44]. CX$_3$CR1-fractalkine interaction may promote the survival and activation of intestine infiltrating donor CD8 T cells. Further studies will reveal the physiological significance of these possibilities.

It has been reported that CXCR6-deficient donor CD8 T cells showed partly reduced infiltration into the liver of GVHR-induced mice on day 7 [45]. Consistent with the previous report, anti-CXCL16 treatment blocked the liver infiltration of CXCR6$^+$ donor CD8 T cells but did not change the overall immunopathology in the liver. In our data, CXCR6 is expressed on a subset of liver-infiltrating donor CD8 T cells on day 14. It remains to be determined which subset of liver-infiltrating donor CD8 T cells express CXCR6 and what role CXCR6$^+$ donor CD8 T cells play during GVHR.

In this study, we demonstrated that the inhibition of the intestinal infiltration of effector donor CD8 T cells could segregate beneficial GVT effects from adverse GVHD. Kim et al. reported that the administration of FTY720, an inhibitor of the sphingosine-1-phosphate receptor, inhibits egression of donor T cells from the lymph nodes, which results in the inhibition of effector donor T cell infiltration into the target organs and alleviates GVHD without impairing GVT effects against lymphoma [46, 47]. However, leukemia and lymphoma cells are not only located in the lymph nodes but are also found in the bone marrow or nonlymphoid tissues. Thus, the egression of effector donor CD8 T cells from secondary lymphoid tissues is thought to be indispensable for optimal GVT effects. In this respect, our approach that interferes with the tissue-specific infiltration of effector donor CD8 T cells could be adapted to a wide range of tumor patients.

In summary, intervention of MAdCAM-1 or fractalkine alleviates intestinal injury and severity of systemic GVHD without hampering GVT effects, suggesting a novel therapeutic approach for the separation of GVT effects from GVHD. It is not claimed that this approach could substitute for the immunosuppressive regimens; however, when used in conjunction with reduced immunosuppressive regimens, it may contribute to make allo-BMT a safe and effective tumor immunotherapy.

ACKNOWLEDGMENTS

REFERENCES

1. Appelbaum, F. R. (2001) Haematopoietic cell transplantation as immunotherapy. *Nature* 411, 385–389.
2. Schleuning, M. (2000) Adoptive allogeneic immunotherapy–history and future perspectives. *Transfus. Sci.* 23, 133–150.
3. Weiden, P. L., Flournoy, N., Thomas, E. D., Prentice, R., Fefer, A., Buckner, C. D., Strob, R. (1979) Antileukemic effect of graft-versus-host disease in human recipients of allogeneic-marrow grafts. *N. Engl. J. Med.* 300, 1068–1073.
4. Horowitz, M. M., Gale, R. P., Sondel, P. M., Goldman, J. M., Kersey, J., Kolb, H. J., Rimm, A. A., Ringden, O., Rozman, C., Speck, B., et al. (1990) Graft-versus-leukemia reactions after bone marrow transplantation. *Blood* 75, 555–562.
5. Storb, R., Deeg, H. J., Pepe, M., Appelbaum, F., Anasetti, C., Beatty, P., Bensinger, W., Berenson, R., Buckner, C. D., Clift, R. (1989) Methotrexate and cyclosporine versus cyclosporine alone for prophylaxis of graft-versus-host disease in patients given HLA-identical marrow grafts for leukemia: long-term follow-up of a controlled trial. *Blood* 73, 1729–1734.
6. Imado, T., Iwasaki, T., Kuroiwa, T., Sano, H., Hara, H. (2004) Effect of FK506 on donor T-cell functions that are responsible for graft-versus-host disease and graft-versus-leukemia effect. *Transplantation* 77, 391–398.
7. Reddy, P., Ferrara, J. L. (2003) Immunobiology of acute graft-versus-host disease. *Blood Rev.* 17, 187–194.
8. Ferrara, J. L., Cooke, K. R., Teshima, T. (2003) The pathophysiology of acute graft-versus-host disease. *Int. J. Hematol.* 78, 181–187.
9. Kunkel, E. J., Butcher, E. C. (2002) Chemokines and the tissue-specific migration of lymphocytes. *Immunity* 16, 1–4.
10. Weninger, W., Manjunath, N., von Andrian, U. H. (2002) Migration and differentiation of CD8$^+$ T cells. *Immunol. Rev.* 186, 221–223.
11. Bradley, L. M. (2003) Migration and T-lymphocyte effector function. *Curr. Opin. Immunol.* 15, 343–348.
12. Wysocki, C. A., Panoskaltsis-Mortari, A., Blazar, B. R., Serody, J. S. (2005) Leukocyte migration and graft-versus-host disease. *Blood* 105, 4191–4199.
13. Panoskaltsis-Mortari, A., Price, A., Hermanson, J. R., Taras, E., Lees, C., Serody, J. S., Blazar, B. R. (2004) In vivo imaging of graft-versus-host-disease in mice. *Blood* 103, 3590–3598.
14. Li, B., New, J. Y., Yap, E. H., Lu, J., Chan, S. H., Hu, H. (2001) Blocking L-selectin and alpha4-integrin changes donor cell homing pattern and ameliorates murine acute graft versus host disease. *Eur. J. Immunol.* 31, 617–624.
15. Petrovic, A., Alpdogan, O., Willis, L. M., Eng, J. M., Greenberg, A. S., Kappel, B. J., Liu, C., Murphy, G. J., Heller, G., van den Brink, M. (2004) LPAM (alpha 4 beta 7 integrin) is an important homing integrin on alloreactive T cells in the development of intestinal graft-versus-host disease. *Blood* 103, 1542–1547.
16. Murai, M., Yoneyama, H., Ezaki, T., Suematsu, M., Terashima, Y., Harada, A., Hamada, H., Asakura, H., Ishikawa, H., Matsushima, K. (2003) Peyer's patch is the essential site in initiating murine acute and lethal graft-versus-host reaction. *Nat. Immunol.* 4, 154–160.
17. Kimura, T., Suzuki, K., Inada, S., Hayashi, A., Isobe, M., Matsuzaki, Y., Tanaka, N., Osuga, T., Fujiwara, M. (1996) Monoclonal antibody against lymphocyte function-associated antigen 1 inhibits the formation of primary biliary cirrhosis-like lesions induced by murine graft-versus-host reaction. *Hepatology* 24, 888–894.
18. Murai, M., Yoneyama, H., Harada, A., Zhang, Y., Vestergaard, C., Guo, B., Suzuki, K., Asakura, H., Matsushima, K. (1999) Active participation of CCR5(+)CD8(+) T lymphocytes in the pathogenesis of liver injury in graft-versus-host disease. *J. Clin. Invest.* 104, 49–57.
19. Serody, J. S., Burkett, S. E., Panoskaltsis-Mortari, A., Ng-Cashin, J., McMahon, E., Matsushima, G. K., Lira, S. A., Cook, D. N., Blazar, B. R. (2000) T-lymphocyte production of macrophage inflammatory protein-1alpha is critical to the recruitment of CD8(+) T cells to the liver, lung, and spleen during graft-versus-host disease. *Blood* 96, 2973–2980.
20. Duffner, U., Lu, B., Hildebrandt, G. C., Teshima, T., Williams, D. L., Reddy, P., Ordemann, R., Clouthier, S. G., Lowler, K., Liu, C., et al. (2003) Role of CXCR3-induced donor T-cell migration in acute GVHD. *Exp. Hematol.* 31, 897–902.
21. Wysocki, C. A., Burkett, S. B., Panoskaltsis-Mortari, A., Kirby, S. L., Luster, A. D., McKinnon, K., Blazar, B. R., Serody, J. S. (2004) Differential roles for CCR5 expression on donor T cells during graft-versus-host disease based on pretransplant conditioning. *J. Immunol.* 173, 845–854.
22. Nestel, F. P., Price, K. S., Seemayer, T. A., Lapp, W. S. (1992) Macrophage priming and lipopolysaccharide-triggered release of tumor necrosis factor alpha during graft-versus-host disease. *J. Exp. Med.* 175, 405–413.
23. Hill, G. R., Ferrara, J. L. (2000) The primacy of the gastrointestinal tract as a target organ of acute graft-versus-host disease: rationale for the use of

cytokine shields in allogeneic bone marrow transplantation. *Blood* **95**, 2754–2759.

24. Mowat. A. M.. Felstein, M. V. (1990) Experimental studies of immunologically mediated enteropathy. V. Destructive enteropathy during an acute graft-versus-host reaction in adult BDF1 mice. *Clin. Exp. Immunol.* **79**, 279–284.

25. Cooke. K. R.. Gerbitz. A.. Crawford. J. M.. Teshima. T.. Hill, G. R.. Tesolin. A.. Possignol. D. P.. Ferrara. J. L. M. (2001) LPS antagonism reduces graft-versus-host disease and preserves graft-versus-leukemia activity after experimental bone marrow transplantation. *J. Clin. Invest.* **107**, 1581–1589.

26. Onai. N.. Kitabatake. M.. Zhang. Y. Y.. Ishikawa, H.. Ishikawa, S.. Matsushima. K. (2002) Pivotal role of CCL25 (TECK)-CCR9 in the formation of gut cryptopatches and consequent appearance of intestinal intraepithelial T lymphocytes. *Int. Immunol.* **14**, 687–694.

27. Fukumoto. N.. Shimaoka, T.. Fujimura. H.. Sakoda. S.. Tanaka, M.. Kita. T.. Yonehara, S. (2004) Critical roles of CXC chemokine ligand 16/scavenger receptor that binds phosphatidylserine and oxidized lipoprotein in the pathogenesis of both acute and adoptive transfer experimental autoimmune encephalomyelitis. *J. Immunol.* **173**, 1620–1627.

28. Nishiyama. Y.. Hamada. H.. Nonaka. S.. Yamamoto. H.. Nanno. M.. Katayama. Y.. Takahashi. H.. Ishikawa, H. (2002) Homeostatic regulation of intestinal villous epithelia by B lymphocytes. *J. Immunol.* **168**, 2626–2633.

29. Yoneyama. H.. Matsuno, K.. Zhang. Y.. Nishiwaki. T., Kitabatake. M.. Ueha, S.. Narumi. S.. Morikawa. S.. Ezaki, T.. Lu. B.. et al. (2004) Evidence for recruitment of plasmacytoid dendritic cell precursors to inflamed lymph nodes through high endothelial venules. *Int. Immunol.* **16**, 915–928.

30. Sale. G. E.. Shulman. H. M.. McDonald. G. B.. Thomas. E. D. (1979) Gastrointestinal graft-versus-host disease in man. A clinicopathologic study of the rectal biopsy. *Am. J. Surg. Pathol.* **3**, 291–299.

31. Lefrancois. L.. Parker. C. M.. Olson, S.. Muller. W.. Wagner. N.. Puddington. L. (1999) The role of beta7 integrins in CD8 T cell trafficking during an antiviral immune response. *J. Exp. Med.* **189**, 1631–1638.

32. Gallatin. W. M.. Weissman. I. L.. Butcher. E. C. (1983) A cell-surface molecule involved in organ-specific homing of lymphocytes. *Nature* **304**, 30–34.

33. Berlin. C.. Berg. E. L.. Briskin. M. J.. Andrew. D. P.. Kilshaw. P. J.. Holzmann. B.. Weissman. I. L.. Hamann, A.. Butcher. E. C. (1993) Alpha 4 beta 7 integrin mediates lymphocyte binding to the mucosal vascular addressin MAdCAM-1. *Cell* **74**, 185–195.

34. Matloubian. M.. David, A.. Engel, S.. Ryan. J. E.. Cyster. J. G. (2000) A transmembrane CXC chemokine is a ligand for HIV-coreceptor Bonzo. *Nat. Immunol.* **1**, 298–304.

35. Imai. T.. Hieshima. K.. Haskell. C.. Baba. M.. Nagira, M.. Nishimura. M.. Kakizaki. M.. Takagi. S.. Nomiyama. H., Schall, T. J.. et al. (1997)

Identification and molecular characterization of fractalkine receptor CX3CR1. which mediates both leukocyte migration and adhesion. *Cell* **91**, 521–530.

36. Wagsater, D., Olofsson. P. S.. Norgren. L., Stenberg. B.. Sirsjo, A. (2004) The chemokine and scavenger receptor CXCL16/SR-PSOX is expressed in human vascular smooth muscle cells and is induced by interferon gamma. *Biochem. Biophys. Res. Commun.* **325**, 1187–1193.

37. Wagsater, D.. Sheikine, Y.. Sirsjo. A. (2005) All-trans retinoic acid regulates CXCL16/SR-PSOX expression. *Int. J. Mol. Med.* **16**. 661–665.

38. Lucas. A. D.. Chadwick. N.. Warren. B. F.. Jewell. D. P.. Gordon. S.. Powrie, F., Greaves. D. R. (2001) The transmembrane form of the CX3CL1 chemokine fractalkine is expressed predominantly by epithelial cells in vivo. *Am. J. Pathol.* **158**, 855–866.

39. Niess, J. H.. Brand, S.. Gu. X.. Landsman, L.. Jung. S.. McCormick. B. A.. Vyas. J. M.. Boes, M.. Ploegh, H. L.. Fox. J. G.. et al. (2005) CX3CR1-mediated dendritic cell access to the intestinal lumen and bacterial clearance. *Science* **307**, 254–258.

40. King. C.. Ilic. A.. Koelsch. K.. Sarvetnick. N. (2004) Homeostatic expansion of T cells during immune insufficiency generates autoimmunity. *Cell* **117**, 265–277.

41. Nishimura. M.. Umehara, H.. Nakayama. T.. Yoneda, O.. Hieshima. K.. Kakizaki. M.. Dohmae. N.. Yoshie. O.. Imai. T. (2002) Dual functions of fractalkine/CX3C ligand 1 in trafficking of perforin+/granzyme B+ cytotoxic effector lymphocytes that are defined by CX3CR1 expression. *J. Immunol.* **168**, 6173–6180.

42. Niess. J. H.. Brand, S.. Gu. X.. Landsman. L.. Jung. S.. McCormick, B. A.. Vyas. J. M.. Boes. M.. Ploegh, H. L.. Fox. J. G.. et al. (2005) CX3CR1-mediated dendritic cell access to the intestinal lumen and bacterial clearance. *Science* **307**, 254–258.

43. Boehme. S. A.. Lio. F. M.. Maciejewski-Lenoir. D.. Bacon, K. B.. Conlon. P. J. (2000) The chemokine fractalkine inhibits Fas-mediated cell death of brain microglia. *J. Immunol.* **165**, 397–403.

44. Sawai. H.. Park, Y. W.. Roberson. J.. Imai. T.. Goronzy. J. J.. Weyand, C. M. (2005) T cell costimulation by fractalkine-expressing synoviocytes in rheumatoid arthritis. *Arthritis Rheum.* **52**, 1392–1401.

45. Sato, T.. Thorlacius. H., Johnston. B.. Staton, T. L.. Xiang. W.. Littman, D. R.. Butcher. E. C. (2005) Role for CXCR6 in recruitment of activated CD8+ lymphocytes to inflamed liver. *J. Immunol.* **174**, 277–283.

46. Matloubian. M.. Lo. C. G.. Cinamon. G.. Lesneski, M. J.. Xu, Y.. Brinkmann. V.. Allende. M. L.. Proia. R. L.. Cyster, J. G. (2004) Lymphocyte egress from thymus and peripheral lymphoid organs is dependent on S1P receptor 1. *Nature* **427**, 355–360.

47. Kim, Y. M., Sachs. T., Asavaroengchai. W., Bronson. R., Sykes, M. (2003) Graft-versus-host disease can be separated from graft-versus-lymphoma effects by control of lymphocyte trafficking with FTY720. *J. Clin. Invest.* **111**, 659–669.